

Wear simulation of automotive engine component materials under biodiesel

S.Y. Cetin¹, M.A. Maleque^{2,*}, H.H. Masjuki¹ and A. Hamdani¹

¹ Department of Mechanical Engineering, International Islamic University Malaysia, 53100, Kuala Lumpur, Malaysia

² Department of Manufacturing and Materials Engineering, International Islamic University Malaysia, 53100, Kuala Lumpur, Malaysia

ABSTRACT – Biodiesel has become increasingly common and significant alternative to traditional petroleum fuel in recent years. However, biodiesel has some adverse effects to the engine components materials. Therefore, in this study, wear simulation of automotive engine component materials was done using computational fluid dynamics approach to develop wear mechanism map. A pin-on-disc configuration was considered as a simulation model of wear under biodiesel using three different types of steel materials whereby load was applied from pin to disc during the simulation process. The relationship between wear rate, applied load and sliding velocity were simulated and discussed followed by a wear mechanism map. The corrosive and abrasive wear mixture were dominated for stainless steel, carbon steel and low-alloy steel. Stainless steel showed more wear-resistant behavior than other materials under biodiesel exposure. The individual wear map generated for the individual material is also discussed in the context of the wear mechanisms observed under biodiesel contact.

ARTICLE HISTORY

Received: 06th June 2022

Revised: 25th July 2022

Accepted: 09th Aug. 2022

Published: 27th Dec. 2022

KEYWORDS

Wear Simulation

Biodiesel

Engine component

Materials

Automotive

Computational fluid dynamics

INTRODUCTION

Wear is defined as an undesired change in the separation of small particles due to mechanical factors that act on the material surface. In contact surfaces, friction forces cause a loss of strength, while wear prevents deterioration of operating tolerances and full function of machine parts. Especially in the automotive industry, selection of the material is crucially important. Chemical reactions between automotive materials and their contact environments directly affect the life and usability of materials. The contact area where fuel is exposed can be deformed due to chemical properties of the fuels that are used in automobiles. Therefore, investigations of automotive materials that are in contact with fuel are of great importance.

Biodiesel is a clean and renewable energy that is produced from the chemical reaction of alcohol and oil. It is a powerful alternative to conventional petroleum diesel due to its low emission and renewable structure. The fundamental difference between diesel and biodiesel is that, although diesel reserves are decreasing, biodiesel is a product that can be continuously renewed by agricultural activities and recycling of household waste oils. Furthermore, biodiesel does not contain petroleum, however it can be used as a fuel in its pure form or by mixing with diesel of petroleum origin in all blending. Biofuel can be derived using any carbonaceous material. Moreover, biodiesel reduces CO₂ emission and decreases the effect of global warming [1]. In other words, biodiesel can reduce smoke by virtue of its short carbon chain and high oxygen content [2]. Besides all its positive properties like low toxicity and low greenhouse gas emissions, it can give rise to environmental damages [3]. Moreover, biodiesel absorbs more water than petroleum diesel fuel. Dissolved water and free water in the structure of biodiesel causes the oxidation of the metallic materials [4]. Besides, acid formation of biodiesel corrodes engine parts [5]. Therefore, various forms of surface problems may occur in the presence of biodiesel [6]. In addition, it is necessary to conduct preliminary testing of engine components under the influence of biodiesel [7]. Arunprasad and Elango [8] explained the friction and wear characteristic of *Navicula* sp. algae biodiesel in RuO₂ concentration. Experiments were performed by 1200 rpm speed and 75 °C of temperature. Looking at the surface structure it was detected that worn parts were excluded from the surface along with the sliding direction. Furthermore, surface degradation reported more than 20 μm which indicates adhesive wear. Singh and Chauhan [9] investigated chrome alloy steel with different blends of biodiesel. To observe the effect of the temperature and load on the surface of the materials, the temperatures 45, 60 and 75 °C and the loads of 147 N and 392 N were applied. Higher surface deformation, adhesive and abrasive wear occurred at high load and temperature.

The simulation studies to be carried out in the wear and tribology field have a great significance in order to predetermine the corrosive behaviour of biodiesel on metal components and to make the appropriate selection of the material. This study contributes to the automotive industry to make a decision about materials which are using for automobiles referring to the findings from this study. Moreover, by the help of this study new simulative analysis was added to the literature. In the present work, the wear behavior of stainless steel, carbon steel and low-alloy steel were simulated under exposure of biodiesel. The pin-on-disc configuration selected as a simulation model. The load and sliding velocity distribution were characterized by computational fluid dynamics (CFD) simulation.

The study shows that it was feasible to simulate wear behaviour of automotive component materials under biodiesel for the prediction of such phenomenon in real life. It is possible to achieve the process parameters for the wear rate with the ANSYS simulation software.

MATERIAL PROPERTIES AND SIMULATION MODEL

In the automotive industry, the suitable material selection is a principle key factor in terms of sustainability and safety. Therefore, three different materials were considered and simulated by the process of this study. Namely, stainless steel, carbon steel and low-alloy steel which are commonly used in automobiles were taken into account as simulation materials. Table 1 presents the chemical composition of stainless steel, carbon steel and low alloy steel. Besides, Table 2 presents the mechanical properties of the selected materials.

Table 1. Chemical Composition of Stainless steel, carbon steel and low-alloy steel [10–12]

Materials/%	C	Mn	Si	P	Cr	Cr	Fe
Stainless Steel 316	0-0.08	0-2	0-1	0-0.045	0-0.03	16.0-18.0	balanced
Carbon Steel (AISI 1065)	0.6-0.7	0.6-0.9	-	0.04	0.05	-	98.31-98.8
Low-alloy Steel (AISI 4140)	0.38-0.43	0.75-1	0.15-0.3	0.035	0.04	0.8-1.1	96.78-97.77

Table 2. Mechanical Properties of stainless steel, carbon steel and low-alloy steel [11–13]

Materials Properties	Stainless Steel	Carbon Steel	Low-alloy Steel
	316	(AISI 1065)	(AISI 4140)
Tensile Strength, MPa	620-795	490	655
Modulus of elasticity, GPa	164	200	190-210
Hardness, Brinell	146	187	197
Poisson's Ratio	0.265-0.275	0.27-0.30	0.27-0.30
Yield Strength, MPa	206	490	415
Bulk Modulus, GPa	134-152	140	140
Shear Modulus, GPa	170-310	80	80

Pre-determination of the simulation materials properties like dimensions and shapes are principal factors that can directly affect the results of the study. In this paper, a pin-disc configuration is used as a simulation model. Moreover, the load applied from pin to disc during the simulation process. Pin was set as a fixed support and the disc was free to move. Besides, Archard's wear model is used in an ANSYS application. Table 3 shows the sizes and dimensions of the materials.

Table 3. Dimension and size of the materials

Properties / Samples	Wear Simulation Specimens	
	Disc	Pin
Outer Diameter (m)	0.10	0.025
Inner Diameter (m)	0.05	-

Creation of friction application is essential for the wear operations. Therefore, the pin-disc configuration is a convenient, practical and simple model to create a desired mechanical friction. Herein, the key function of the pin is to create continuous friction on the disc surface. In other respects, a biodiesel liquid environment was created and interworked with a pin-disc model. Figure 1 shows the pin-on-disc configuration with a biodiesel environment.

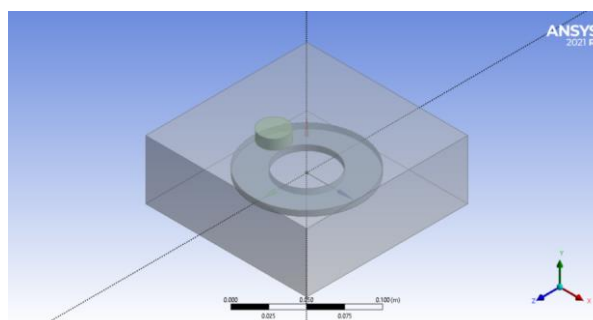


Figure 1. Pin-on-disc configuration with palm biodiesel environment

In CFD software, meshing is necessary before running the simulation. The reason for the meshing is to break down a complex volume into small pieces where the simulation is performed. Specifically, mesh can be defined as a network of cells and dots. The size and shape of the mesh may vary from user to user which perform the simulation. Some of the important factors that affect meshing are; converge for better response using suitable tolerance limit and shape of the material, allowance of material disfigurement within acceptable limits, making a decision about which edges to divide into and how many parts to be divided into etc. The 3D model is meshed by a size of 3 mm that provides fine mesh. Figure 2 shows the meshed geometry of pin-disc configuration.

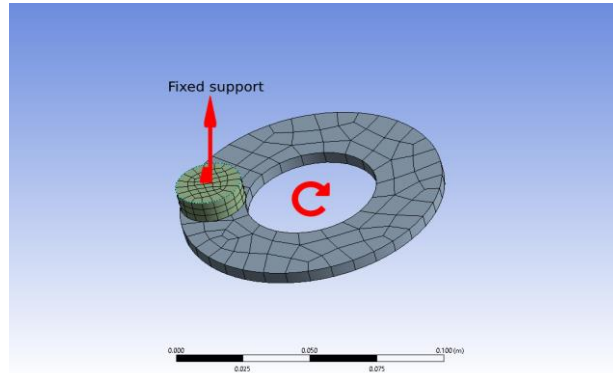


Figure 2. Meshed geometry of pin-disc configuration

Biodiesel Properties

The proper geometry of the liquid box was designed and the selected material was applied. The liquid part of this simulation study is decided on palm biodiesel with the properties that are shown in Table 4. For teasy computation, 1 m/s velocity is considered to be the liquid.

Table 4. The properties of palm biodiesel [14]

Properties/Fluent	Palm Biodiesel
Density (kg/m^3)	880
Specific Heat (J/kg.K)	2193.27
Thermal Conductivity (W/m.K)	0.1157
Viscosity (kg/m.s)	0.049
Flash point ($^{\circ}\text{C}$)	164

Biodiesel entered at a velocity of 1 m/s from the inlet section and left the system from the outlet section as shown in Figure 3. Flow conditions provided ease of calculation. Furthermore, calculations performed for stainless steel, carbon steel and low-alloy steel separately. Here the solution was made by adding data transferred from fluent. Figure 3 shows the setup stage of the simulation system.

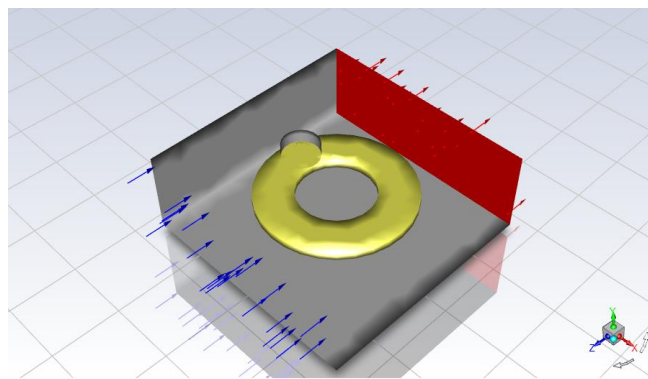


Figure 3. Setup stage of the simulation system

Boundary Conditions

To get high accuracy simulation results, specifying boundary conditions as close as actual experimental working conditions are essential. Pin was identified as a fixed support and disc was free to move. Simulation materials were applied and simulated to the disc on an individual basis. The liquid was defined as the palm biodiesel. Besides, the environmental

temperature of 25 °C was defined as a reference temperature. The applied load from pin to disk was defined between 0-80 N. In other flipside, the sliding velocity changed from 0 m/s to 10 m/s. The simulation was performed using the ANSYS 2021. The turbulent flow was associated with every control volume and solved with program controlled iterations.

RESULTS AND DISCUSSION

Wear Behaviour of Materials Under Biodiesel

Wear mechanism can be affected by some basic parameters, such as sliding velocity, load and sliding distance. Principally, the worn volume (V) is directly proportional by applied load (F_N) as seen in Eq. (1) [15]. Moreover, the relationship between material hardness (H_s), sliding distance (L), material density (γ) and weight loss (G) are also definable according to the following equation;

$$V = \frac{k_0 F_N L}{H_s} = \frac{G}{\gamma} \quad (1)$$

The equation was employed in the simulation in order to find out the relationship between applied load and wear rate starting from the applied load of 0 N and continued till applied load of 80 N as ramped. According to the simulation results, for all three materials (as shown in Figure 4), similar wear rate reactions were spotted against the increased load. Wear rates escalated until 30 N of applied load for all three samples. Afterwards, almost steady state wear was observed with the increasing of the applied load in the simulation. It can be seen that the highest wear rate for stainless steel, carbon steel and low-alloy steel was $1.26 \times 10^{-2} \text{ mm}^3/\text{Nm}$, $1.28 \times 10^{-2} \text{ mm}^3/\text{Nm}$ and $1.32 \times 10^{-2} \text{ mm}^3/\text{Nm}$, respectively.

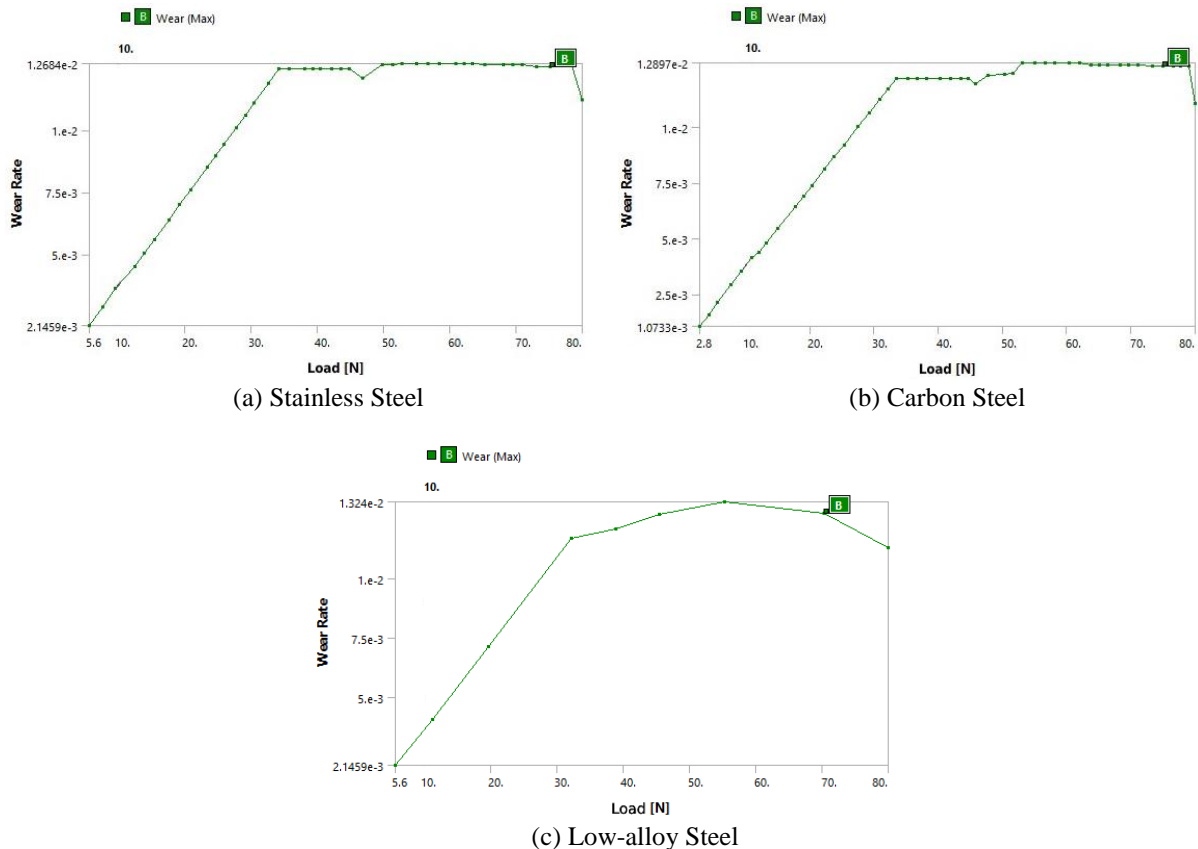


Figure 4. Wear rate-load graphs of stainless steel, carbon steel and low-alloy steel

Considering the impact of load, it was observed that wear rate dramatically increased up to 30 N load. Afterwards, almost stationary condition was detected along with the load increases. At the 80 N of applied load, the wear rate moderately reduced by the decrease of sliding velocity. Figure 5 presents the graphs of wear rate and sliding velocity of the materials. The wear rate of all three materials showed an increasing trend with the increasing of sliding velocity under biodiesel. It was also noticed that wear rate significantly increased linearly up to 3.75 m/s sliding velocity. However, maximum wear rate of stainless steel, carbon steel and low-alloy steel was recorded at 6.60 m/s, 7.61 m/s and 6.5 m/s of sliding velocities, respectively. The lower wear rate was observed for stainless steel material compared to other two materials. However, a similar wear behavior was noticed when compared with a study that does not use biodiesel but had a surface coating on the stainless steel [16]. This action provided a message on the impact of biodiesel on metal

components. The improvement in wear behavior without the use of surface coating indicates that biodiesel increases wear resistance within the short term. On the other hand, the wear rate of low-alloy steel increased with the increasing of the applied load but similar to carbon steel and stainless steel as shown in Figure 5. Low-alloy steel portrayed its maximum wear rate between 50 N and 60 N, and showed the highest wear rate compared to stainless steel and carbon steel. Sliding velocity is the significant parameter that directly affects to the wear phenomena [17].

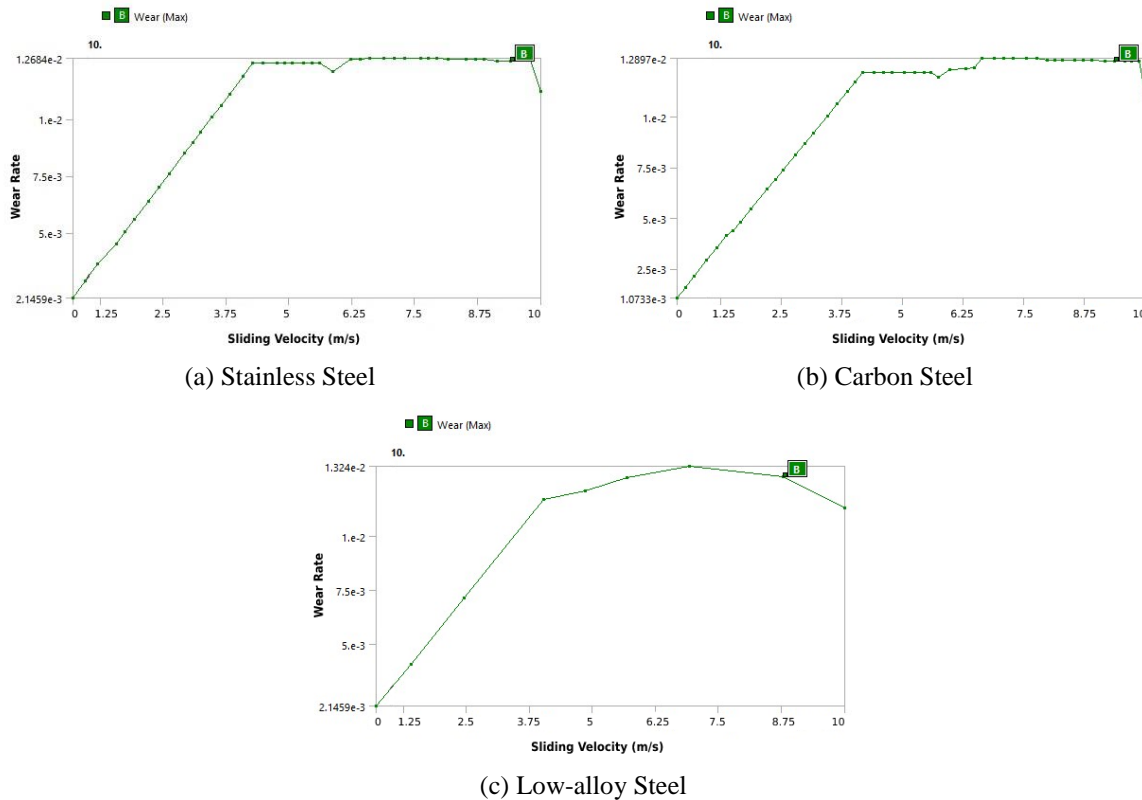


Figure 5. Wear rate-sliding velocity graphs of stainless steel, carbon steel and low-alloy steel

When compared to previous studies [16], it was noticed that the wear behaviour of stainless steel which was examined without surface coating showed close results to the surface coated stainless steel. This behaviour clearly illustrates the effect of biodiesel on metal components. In other words, it is known that surface coatings are used due to their wear preventing behaviour on metal components. However, in this study, the wear rate of the metals reduced although there was no surface coating, which indicates that biodiesel plays a role in reducing wear on metals in short-term interactions.

The reason of the decrease in wear rate after a particular load may be due to the formation of a protective layer on the material surfaces. This protective film layer which is caused by biodiesel plays a reducing role in the wear of the material surfaces [18]. According to Soydan et al. [19] boronized and Fe₂B surface coated AISI 4140 type of low alloy steel showed a wear rate of 6×10^{-4} mm³/Nm by pin-disc configuration. In addition, the constant load of 30 N was applied from pin to disc. In other research, the nitride AISI 4140 low alloy steel showed 6×10^{-6} mm³/Nm. Furthermore, the least wear rate was observed in a short time period due to the effect of nitrogen diffusion [20]. As a healthy comparison, in the present study, when looking at the wear rate at the applied load of 30 N, it was observed that the recorded wear rate was 1.17×10^{-2} mm³/Nm. It is clearly seen that there was a significant difference compared to the data in previous studies. There may be several reasons for the difference between obtained wear rates. Surface coating is one of the main factors that affect the wear rate of the material. Besides, biodiesel can trigger wear on the surface. In order to make more accurate comparisons for AISI 4140 low alloy steel, further studies are needed by making surface coatings and changing the simulation environment.

Wear Mechanism Map

The graphical representation of the interfacial conditions (sliding velocity, load, time, sliding distance etc.) can be presented as a wear map which can help to identify the degradation conditions and optimize forming process of the material [21]. Wear map mainly demonstrates a particular type of wear that is dominant under interfacial conditions during the process of wear. As mentioned in the previous section, wear rate increased with the increasing of both sliding velocity and applied load. Also mentioned that all three simulated materials have shown a close wear behavior. Therefore, the individual wear maps were developed in this study for all material individually as shown in Figure 6. The mixture of corrosive and abrasive wear were dominated on the surface of all materials. However, it is worthy to mention that better

wear-resistant behavior was observed on the surface of stainless steel compared to two materials such as carbon steel and low-alloy steel.

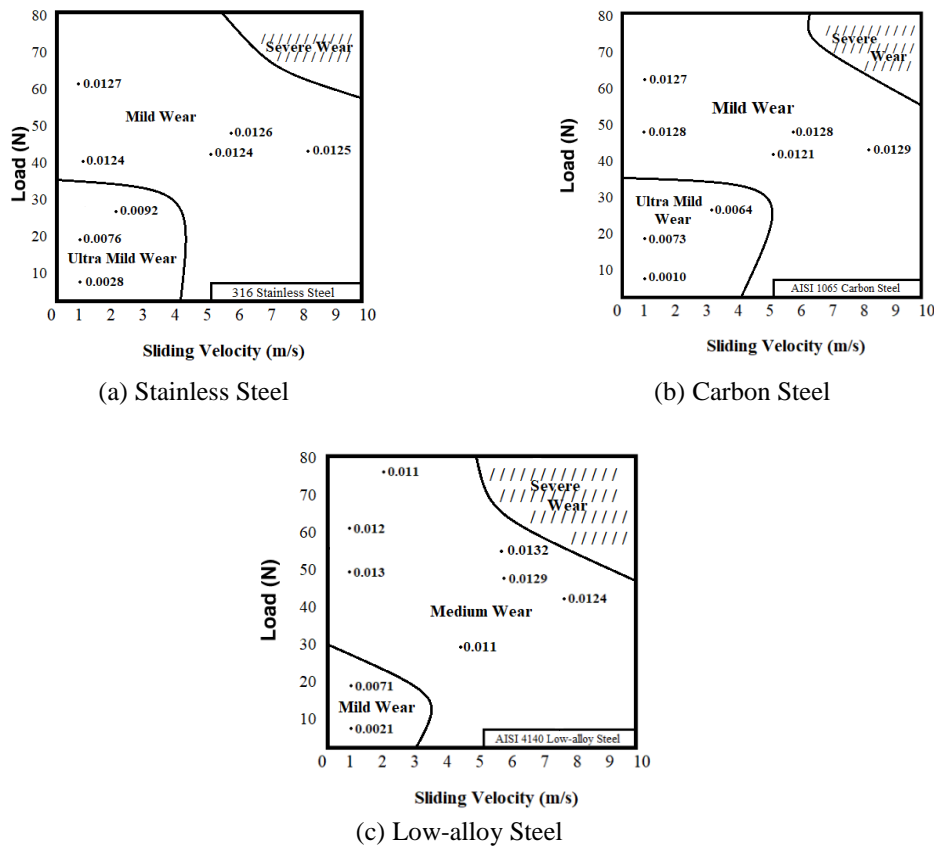


Figure 6. Wear mechanism maps of stainless steel, carbon steel and low alloy steel

Wear Mechanism Map of Pin-on-disc Configuration for Steel

In this present study, a normalized wear mechanism map of pin-on-disc configuration for steel was shown on the wear mechanism maps that developed by Lim and Ashby [22] in Figure 7. They present various types of wear mechanisms that involved for a particular type of metallic steel under a normalized pressure and normalized velocity. Therefore, the sliding velocity and normal applied load of the present work were converted to normalized load and normalized velocity which is again in line with the guideline of Lim and Ashby wear map. The normalized load and normalized velocity were calculated according to the Eqs. (2) and (3) [22]. Herein, H_0 is the hardness at the room temperature, A_n is the contact area of the wear surface, F is applied load, r_0 is radius of the contact area, a is the thermal diffusivity and \tilde{v} is velocity.

$$\tilde{F} = \frac{F}{A_n H_0} \tag{2}$$

$$\tilde{v} = \frac{v r_0}{a} \tag{3}$$

After normalization, the obtained values are:

- Sliding velocity of 0 - 10 m/s showed the normalized value of 0 - 6.5×10^4
- Normal load of 0 - 80 N showed the normalized value of 0 - 1.44×10^{-5}

where, average hardness of stainless steel, carbon steel and low-alloy steel is 176, thermal diffusivity is $9.1 \times 10^{-6} \text{ m}^2 \cdot \text{s}^{-1}$.

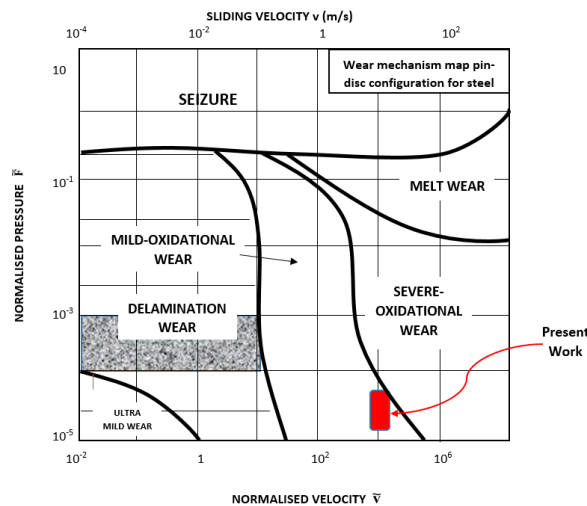


Figure 7. Wear mechanism map of pin-on-disc configuration for steel [22]

In the present study, mild corrosive and abrasive types of wear were observed within the regime of mild-oxidational wear in the graph (Figure 7). Oxidative wear is one of the co-definition of chemical wear where oxygen is dominant whereas corrosive or chemical wear occurs by virtue of friction in a corrosive environment. Corrosion, in between surface and environment, can occur by the reason of chemical or electrochemical reactions [23]. Therefore, in this study, corrosive and/or oxidative wear is mainly caused by biodiesel and mild abrasive wear is mainly due to frictional interaction of pin-on-disc configuration. The wear process can be categorized into the low wear, mild wear and severe wear [24]. As mentioned earlier, mild wear was observed with lower sliding velocities and loads and it is in agreement with the work done by [25]. As similar to load-wear rate relation, the wear rate increased with the increase of sliding velocity. Finally, it can be concluded that the wear regime for steel materials is in the mild-oxidative wear regime and also biodiesel can control the wear resistance of automotive engine component materials that were considered in the simulation study.

CONCLUSION

Wear simulation of automotive engine component materials was successfully done using computational fluid dynamics approach and a wear mechanism map was developed. Wear simulation results showed that stainless steel was the most resistant material as it showed the least wear rate value of $1.2684 \times 10^{-2} \text{ mm}^3/\text{Nme}$. On the other hand, low-alloy steel was observed less resistant than carbon steel and the wear rate value was $1.324 \times 10^{-2} \text{ mm}^3/\text{Nm}$ and $1.2807 \times 10^{-2} \text{ mm}^3/\text{Nm}$, respectively. The wear rates of all three materials dramatically increased until 30 N of applied load and then exhibited almost steady state wear rate with the increasing of the applied load in the simulation. Correlatively with the load increase, wear rate increased with the sliding velocity increases. However, maximum wear rate of stainless steel, carbon steel and low-alloy steel was recorded at 6.60 m/s, 7.61 m/s and 6.5 m/s of sliding velocities, respectively. Finally, the wear regime for steel materials demonstrated in the mild-oxidative wear regime even under biodiesel condition which can control the wear resistance of automotive engine component materials. The simulation contributes to the automotive industry to make a decision on appropriate and suitable material selection which are in contact with biodiesel.

ACKNOWLEDGEMENT

The authors would like to acknowledge to the Malaysian Tribology Society (MYTRIBOS) for funding this research through project No. MIG-0005-2021 and also to the International Islamic University of Malaysia (IIUM) for technical supports that made this study possible.

REFERENCES

- [1] S. Firoz, "A review: Advantages and disadvantages of biodiesel," *International Research Journal of Engineering and Technology*, vol. 4, no. 11, pp. 530–533, 2017.
- [2] M. Setiyo, D. Yuvenda, and O.D. Samue, "The concise latest report on the advantages and disadvantages of pure biodiesel (B100) on engine performance: Literature review and bibliometric analysis," *Indonesian Journal of Science & Technology*, vol. 6, no. 3, pp. 469–490, 2021.
- [3] N. Nasir and Z. Daud, "Performance of aluminium Sulphate and Polyaluminium Chloride in biodiesel wastewater," *Journal of Mechanical Engineering and Sciences*, vol. 7, no. 1, pp. 1189–1195, 2014.
- [4] T. Suthisripok and P. Semsamran, "The impact of biodiesel B100 on a small agricultural diesel engine," *Tribology International*, vol. 128, pp. 397–409, 2018.

- [5] G. Sriram and A. Kumar, "Evaluation of performance of crankcase oil in a biodiesel engine - A case study," *Tribology Online*, vol. 6, no. 5, pp. 235–238, 2011.
- [6] A. Maleque and A. A. Abdulmumin, "Tribocorrosion behaviour of biodiesel; A review," *Tribology Online*, vol. 9, no. 1, pp. 10–20, 2014.
- [7] L. Gil, D. Pieniak, E. Kozłowski, and J. Selech, "Impact of selected biofuels and diesel as lubricants on the statistical distribution and course of sliding friction coefficients for the kinematic pair 100Cr6-100Cr6," *Tribologia*, vol. 288, no. 6, pp. 17–23, 2019.
- [8] J. Arunprasad and T. Elango, "Tribological behaviour of RuO₂ in diesel: Benthic-diatom *Navicula* sp. algae biodiesel," *Indian Journal of Geo-Marine Sciences*, vol. 49, no. 08, pp. 1473–1478, 2020.
- [9] P. Singh, Varun, and S. R. Chauhan, "Influence of temperature on tribological performance of dual biofuel," *Fuel*, vol. 207, pp. 751–762, 2017.
- [10] P. Bharath, V. G. Sridhar, and M. S. kumar, "Optimization of 316 stainless steel weld joint characteristics using Taguchi technique," *Procedia Engineering*, vol. 97, pp. 881–891, 2014.
- [11] AISI 1065 Carbon Steel (UNS G10650), <https://www.azom.com/article.aspx?ArticleID=6575> (accessed Nov. 30, 2022).
- [12] AISI 4140 Alloy Steel (UNS G41400), <https://www.azom.com/article.aspx?ArticleID=6769> (accessed Nov. 30, 2022).
- [13] 316 Stainless Steel Mechanical Properties, <https://www.ezlok.com/316-stainless-steel-properties> (accessed Nov. 30, 2022).
- [14] Z. Taghizade, "Determination of biodiesel quality parameters for optimization of production process conditions," *Master Thesis*, Polytechnic Institute of Bragança, Portugal, 2016.
- [15] D. Odabas, "Effects of load and speed on wear rate of abrasive wear for 2014 Al alloy," *IOP Conference Series: Materials Science and Engineering*, vol. 295, p. 012008, 2018.
- [16] M. Lepule, B. Obadele, A. Andrews, and P. Olubambi, "Corrosion and wear behaviour of ZrO₂ modified NiTi coatings on AISI 316 stainless steel," *Surface and Coatings Technology*, vol. 261, pp. 21–27, 2015.
- [17] M. Yin, Z. Cai, Y. Yu, and M. Zhu, "Impact-sliding wear behaviors of 304SS influenced by different impact kinetic energy and sliding velocity," *Tribology International*, vol. 143, p. 106057, 2020.
- [18] E.S. Almeida, F.M. Portela, R.M.F. Sousa, D. Daniel, M.G.H. Terrones, E.M. Richter, and R.A.A. Muñoz, "Behaviour of the antioxidant tert-butylhydroquinone on the storage stability and corrosive character of biodiesel," *Fuel*, vol. 90, no. 11, pp. 3480–3484, 2011.
- [19] Y. Soydan, S. Koksall, A. Demirer, and V. Celik, "Sliding friction and wear behavior of pack-boronized AISI 1050, 4140, and 8620 steels," *Tribology Transactions*, vol. 51, no. 1, pp. 74–81, 2008.
- [20] A. Alsaran, F. Yildiz, and A. Celik, "Effects of post-aging on wear and corrosion properties of nitrided AISI 4140 steel," *Surface and Coatings Technology*, pp. 3147–3154, 2006.
- [21] R. Ramachandran, "Machine learning model to map tribocorrosion regimes in feature space," *Coatings*, vol. 11, no. 4, p. 450, 2021.
- [22] S. C. Lim and M. F. Ashby, "Overview no. 55 wear-mechanism maps," *Acta Metallurgica*, vol. 35, no. 1, pp. 1–24, 1987.
- [23] C. Zhang, "Understanding the wear and tribological properties of ceramic matrix composites," *Advances in Ceramic Matrix Composites (Second Edition)*, Woodhead Publishing Series in Composites Science and Engineering, pp. 401–428, 2014.
- [24] R. Aghababaei, T. Brink, and J. Molinari, "Asperity-level origins of transition from mild to severe wear," *Physical Review Letters*, vol. 120, no. 18, p. 186105, 2018.
- [25] M. Sharma and R. Sehgal, "Dry sliding friction and wear behaviour of Titanium alloy (Ti-6Al-4V)," *Tribology Online*, vol. 7, no. 2, pp. 87–95, 2012.